Chemical Engineering Journal 214 (2013) 189–197

Contents lists available at SciVerse ScienceDirect

Chemical Engineering Journal

journal homepage: www.elsevier.com/locate/cej

Removal of lead(II) from aqueous solution with ethylenediamine-modified yeast biomass coated with magnetic chitosan microparticles: Kinetic and equilibrium modeling

Ting-ting Li [a,b], Yun-guo Liu [a,b,*], Qing-qing Peng [a,c,d], Xin-jiang Hu [a,b], Ting Liao [a,b], Hui Wang [a,b], Ming Lu [a,b]

[a] *College of Environmental Science and Engineering, Hunan University, Changsha 410082, PR China*
[b] *Key Laboratory of Environmental Biology and Pollution Control, Hunan University, Ministry of Education, Changsha 410082, PR China*
[c] *Hunan Environmental Monitoring Centre, Changsha 410019, PR China*
[d] *Key Laboratory of State Environmental Protection and Heavy Metal Pollution Monitoring, Changsha 410019, PR China*

HIGHLIGHTS

- ▶ The EYMC is an excellent adsorbent for the removal of Pb(II) ions.
- ▶ The EYMC can be separated from reaction medium easily.
- ▶ The experiment data fitted best with Langmuir and pseudo-second-order models.
- ▶ The adsorption showed a spontaneous and endothermic adsorption process.
- ▶ EYMC was regenerated successfully and only lost 0.61 mg g^{-1} after four cycles.

ARTICLE INFO

Article history:
Received 11 August 2012
Received in revised form 28 October 2012
Accepted 29 October 2012
Available online 7 November 2012

Keywords:
Biosorption
Lead(II)
Kinetic
Equilibrium isotherm

ABSTRACT

The adsorption of Pb(II) ions from aqueous solution with ethylenediamine-modified yeast biomass coated with magnetic chitosan microparticles (EYMC) was studied in batch adsorption system. The adsorption of Pb(II) ions increased with the rising pH and a higher adsorption capacity was achieved at the pH 4.0–6.0. The experiment data was well matched by Langmuir model and Freundlich model, while Langmuir model showed the best description. The maximum adsorption capacities obtained by Langmuir model were 121.26, 127.37 and 134.90 mg g^{-1} at 20, 30 and 40 °C, respectively. Kinetic studies indicated that the pseudo-second-order model was appropriate to describe the adsorption process and film diffusion maybe governed the rate of the adsorption. Thermodynamic studies revealed that a spontaneous and endothermic adsorption process. The adsorbents, EYMC can be well recovered by 0.1 M EDTA.

1. Introduction

The release of lead has recently attracted great attention because of its widespread adoption, toxic effects, accumulation in living tissues and adverse impact on human health [1]. Therefore, disposal of metal ions from source water is necessary before discharging into the environment. Innovative and improved methods have developed to remove metal ions from metal-laden wastewater, such as chemical precipitation, ion exchange, electrolysis, coagulation, membrane separation, reverse osmosis processes, and adsorption [2]. However, great challenges are faced by these methods due to the technological problems, ineffectiveness at low metal concentration and high cost [3]. Biosorption is considered as one of the promising technologies and has been continuously studied in recent years. A variety of living and dead microorganisms or biomaterials, such as bacteria, fungi, algae, yeast, and mosses have been proved their credibility in dilute metal ions [4–6]. Since no growth media or nutrients are required, the use of dead cells has more advantages than living cells. Moreover, dead cells have lower sensitivity to the pollutant concentration and an easy mathematical modeling [7]. In the practical application of industrial operation, immobilization is regarded as an effective method to improve the applicability of the adsorbents. This technique provides the superiorities of improved mechanical strength, good performance, rigidity and porosity characteristics to the

---

* Corresponding author at: College of Environmental Science and Engineering, Hunan University, Changsha 410082, PR China. Tel.: +86 731 88649208; fax: +86 731 88822829.

E-mail address: yunguoliu12@163.com (Y.-g. Liu).

1385-8947/$ - see front matter © 2012 Elsevier B.V. All rights reserved.
http://dx.doi.org/10.1016/j.cej.2012.10.055

adsorbents [8]. Moreover, the processes of adsorption are more competitive and economic for their easy operation of repeating adsorption–desorption cycles [9].

The choice of adsorbent is not only determined by their sorption capability, kinetic parameters but also by their price and reusability. The overall economic is mainly influenced during the choice of experimental biomass [10]. Yeast is widely used in the field of fermentation, bread production and xylitol production. According to the various studies yeast biomass can chelate copper, lead, cadmium, mercury and methyl violet to the amino and hydroxyl groups of the biomass surface [11,12]. The enhancement of the biosorption capacity is presently practicable by several techniques, including the heat treatment, freeze drying, acids, alkalis, and organic chemicals [13,14]. The biosorption capacity was efficiently improved by the selective modification of *Rhizopus niqricans* [15]. Moreover, according to Volesky et al. [13] the removal of cadmium from metal-laden water is currently feasible thanks to dried yeast.

A quantity of synthetic polymers was used in order to immobilize microbe. The choice of chitosan is due to its reactive groups (amino and acetamido), excellent ability to chelate resins, high hydrophilicity, biodegradability and ease of chemical derivatization. In addition, chitosan has been proved environmental friendly [16]. Nevertheless, chitosan solubility at low pH is poor. In order to improve the stability in acid solutions, many cross-linking agents such as glutaraldehyde, glyoxal, and epichlorohydrin were used [16,17].

Traditional methods of separation after adsorption are filtration, sedimentation and centrifugation. Yet they may inefficient and uneconomical. The problem is easily resolved by magnetic materials. Magnetic carriers serve as supporting materials for adsorbents and they are easily separated from the aqueous solutions by an external magnet [18].

The ability of eliminating metal ions from solutions is influenced by the number of available reactive groups on the material surface. In order to increase the adsorption capability, various chitosan derivatives, such as glycine, polydimethylsiloxane, and thioureaandmaleic anhydride are used [17,19].

This work focused on the sorption of Pb(II) by ethylenediamine-modified yeast biomass coated with magnetic chitosan microparticles (EYMC). Variable effects including initial pH, temperature, initial Pb(II) concentration, contact time and desorption properties were considered. In order to investigate the mechanism of the sorption, the collected experiment data was fitted to kinetic and equilibrium models. In order to compare the capability of the sorbents, the other three sorbents (yeast biomass coated with magnetic chitosan microparticles (YMC), ethylenediamine-modified magnetic chitosan microparticles (EMC) and magnetic chitosan microparticles (MC) were prepared and used as the control group.

2. Materials and methods

2.1. Materials

Chitosan (90% acetylation degree) was supplied by Sinopharm Chemical Reagent Co. Ltd., Shanghai, China. Glutaraldehyde and epichlorohydrin were provided by Tianjin Guangfu Fine Chemical Research Institute, Tianjin, China. Ethylenediamine was obtained from Changsha Subintersection Plastic Chemical Factory, Changsha, China. Ferric chloride-6-hydrate and ferrous chloride-4-hydrate were purchased from Tianjin Kermel Reagent Co. Ltd., Tianjin, China. The yeast was purchased from Hunan Normal University. Stock solutions of lead(II) were prepared by dissolving $Pb(NO_3)_2$, obtained by Sanpu Chemical Reagent Co. Ltd., Shanghai, China. All the reagents were of analytical grade. Distilled water was provided from a distilled water system, purchased from Shanghai Boxun Co. Ltd., China.

2.2. Preparation of magnetic fluid

Magnetic fluid was prepared according to the method reported by Bao et al. [20]. Under the protection of N_2, $FeCl_2{\cdot}4H_2O$ and $FeCl_3{\cdot}6H_2O$ (molar ratio 1:2) were dissolved in water, then the resulting solution was precipitated by adding NaOH.

2.3. Preparation of EYMC and control group

EYMC was prepared by the following steps: first, adding the yeast suspension into the chitosan solution (1% w/v) and stirring at 30 °C for 12 h. Chitosan solution (1% w/v) was prepared by dissolving 1.0 g chitosan in 100 mL of 1% (v/v) acetic acid. Second, magnetic fluid was then injected into the reaction system and transferred into the boiling flask-3-neck. Third, 10 mL glutaraldehyde (4% v/v) was added into the system to form the particles after ultrasonic dispersion. Fourth, 12 mL ethylenediamine (purity 99%) was introduced into the mixture to modify active groups to the particles. Then the EYMC was collected by an external magnet. The resultant precipitate was finally dried by placing them in the Vacuum freeze dryer.

The synthetic method of MC, EMC and YMC was similar to the preparation of EYMC. In the whole process, EMC was produced with the absence of yeast suspension. If the synthetic process just included the first three steps, with the addition of yeast suspension, the particle was YMC; while without it, the product was MC.

2.4. Characteristic analysis

The characteristic of EYMC before and after adsorption was analyzed by the following techniques. The surface morphology of EYMC was observed by Hitachi TM 3000. The FTIR spectrum was taken by the usage of Varian 3100 FT-IR with a background spectrum measured on pure KBr. Surface area was determined by N_2 adsorption–desorption isotherm using Beckman Coulter SA3100. The Pb(II) concentration was measured at the radiation of lead atoms of 283.8 nm by Atomic adsorption spectrometer (PerkinElmer AA700, detection limit for lead is 0.03 mg L^{-1}).

2.5. Batch adsorption and desorption experiments

Batch experiments were carried out with adsorbents in a 100 mL Erlenmeyer flask containing 25 mL Pb(II) solutions on a shaker at 150 r min^{-1}. For each treatment, 25 mg adsorbent was added and agitated for an appropriate period. The concentrations of Pb(II) were determined by the Atomic adsorption spectrometer.

Four kinds of adsorbents (EYMC, MC, EMC, and YMC) were used to study the pH and temperature effect on Pb(II) ions adsorption, while the last three were used as control group. Effects of pH (2.0–6.5) experiments were studied in 25 mL Pb(II) solutions with the initial concentration of 50 mg L^{-1} at a temperature of 30 °C. Effect of temperature was investigated at the initial concentration of 50 mg L^{-1} with different temperatures of 20, 30, 40 °C, respectively. The pH was initially adjusted by 1 mol L^{-1} NaOH and HCl and not controlled during the experimentation.

Isotherm studies were carried out with different initial Pb(II) concentrations (at the range of 10–500 mg L^{-1}) by contacting 25 mg EYMC for 1 h. The experiments were conducted at different temperatures of 20, 30 and 40 °C, respectively. The amount of Pb(II) ions bounded by the adsorbent was calculated according to the following equation:

$$q_e = \frac{(C_0 - C_e)V}{m} \quad (1)$$

where q_e is the amount of metal ions adsorbed per weight unit of adsorbent after equilibrium (mg g^{-1}). C_0 and C_e are the initial and equilibrium concentration in the solution (mg L^{-1}). V is the volume of metal solution (L) and m is the weight of the adsorbent (g).

Kinetic experiments were investigated by shaking the flasks in different contact time (0–240 min). For each experiment, 25 mg EYMC was added to 25 mL Pb(II) ions solution with different initial concentration of 30, 50, 100 mg L^{-1}.

To validate the reusability of the EYMC, the adsorption–desorption cycles were repeated continuously for four times. For each adsorption–desorption cycle, after adsorption process (initial concentration, 50 mg L^{-1}; absorbent dose, 25 mg; contact time, 1 h; volume, 25 mL; temperature, 30 °C; pH value, 5.5; agitation speed, 150 r min^{-1}) EYMC adsorbed with Pb(II) was separated from the solution by placing the flask on a magnet. Then they were added into 25 mL 0.1 M EDTA (as desorption solution). The flasks were stirred at 30 °C with the speed of 150 r min^{-1} for another 1 h. The concentrations of metal ions were analyzed. EYMC was washed three times by the distilled water before its succeeding cycle. The desorption ratio of Pb(II) by EDTA was calculated as follows:

$$\text{Adsorption efficiency } (\%) = \frac{C_0 - C_e}{C_0} \times 100 \quad (2)$$

$$\text{Desorption } (\%) = \frac{C_d}{C_a} \times 100 \quad (3)$$

where C_0 and C_e are the initial and equilibrium concentration in the solution (mg L^{-1}). C_d is the amount of Pb(II) ions desorbed to the EDTA solution (mg g^{-1}). C_a is the amount of Pb(II) ions adsorbed onto the EYMC (mg g^{-1}).

3. Results and discussion

3.1. Surface morphology of EYMC

Surface morphology of the EYMC before and after adsorption was investigated by SEM. As shown in Fig. 1a, the SEM image indicated primordial EYMC was an adsorbent with rough surface, the surface area of EYMC was found by N_2 adsorption–desorption isotherm (13.2 m^2 g^{-1}). There are many small bumps on the surface of EYMC and they form a large quantity of pores. These may significantly contribute to the transfer of Pb(II) ions to the surface of the adsorbent. After adsorption in Fig. 1b, the pores were adhered by lead. This proved that the Pb(II) ions can be easily absorbed by the EYMC.

3.2. FTIR spectroscopy

The FTIR spectra of MC, EYMC and EYMC-Pb were shown in Fig. 2a–c. For the MC (Fig. 2a), the wide band at 3300 cm^{-1} was clearly and corresponded to the overlapping of —NH/—OH stretching [21,22]. The characteristic peak of chitosan shown at 2870 cm^{-1} was due to the stretching vibration of —CH and —CH_2. The adsorption peak at about 1660 cm^{-1} and 1563 cm^{-1} were assigned to the C=O and N—H/C=O combination of the amide II bond, indicating the presence of carboxyl groups [23]. The peaks at 1061 cm^{-1} were related to the combined effects of C—N stretching vibration of primary amines and the C—O stretching vibration from the primary alcohol in chitosan [22]. The bands round at 590 cm^{-1} were assigned to Fe—O bond vibration, which indicates the presence of Fe_3O_4 as a result of the successful coating procedure. Because the surface of iron oxide with negative charges has an affinity toward chitosan, protonated chitosan could coat the magnetite particles by the electrostatic interaction and chemical reaction through glutaraldehyde crosslinking [24].

Compared with Fig. 2a and b, the intensity of the peak at 3300 cm^{-1} (overlapping of —NH/—OH stretching) strengthened and the peak shifted to 3375 cm^{-1}. The narrowed peak of N—H bending vibration at 1563 cm^{-1} and C—N stretching vibration at 1061 cm^{-1} were probably due to the more amine groups modified to the EYMC. The peak 1660 cm^{-1} relating to the stretching vibration of C=O shifted to 1674 cm^{-1}, also the intensity was strengthened, may due to the immobilization of yeast biomass.

After adsorption (Fig. 2c), it was observed from the spectra that the peak of overlapping of —NH/—OH stretching vibration shifted to 3458 cm^{-1}, indicating that —OH joined in the coordination with Pb(II). The peak of C=O at 1674 cm^{-1} was weak after adsorption and the peak position shifted to 1682 cm^{-1}. A decrease in intensity of the N—H bending vibration at around 1563 cm^{-1} was also observed. These results indicated that the hydroxyl groups, carboxyl groups and amino groups play an important role in Pb(II) ions removal.

3.3. Effect of pH

In this study, effect of pH was investigated at the range of 2.0–6.5. The effects of pH on MC, EMC, YMC and EYMC were displayed in Fig. 3. As shown in Fig. 3, the highest adsorption capacity of EYMC was evident, compared with the others, and available in a wide range of pH. The maximum adsorption amounts decreased in the order of EYMC > EMC > YMC > MC. The curve of EYMC was smoother (at the range of 4.0–6.5) than the other three and it revealed similar adsorption capacity of Pb(II) ions. These results indicated that pH played an important role on the adsorption process.

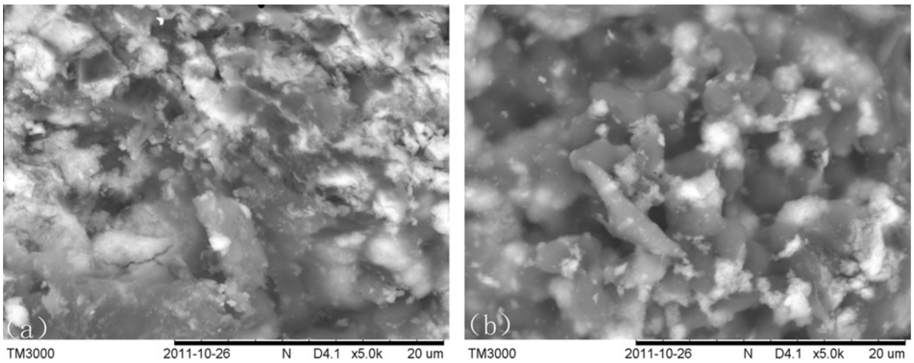

Fig. 1. The SEM images for EYMC before (a) (5000×) and after (b) (5000×) adsorption.

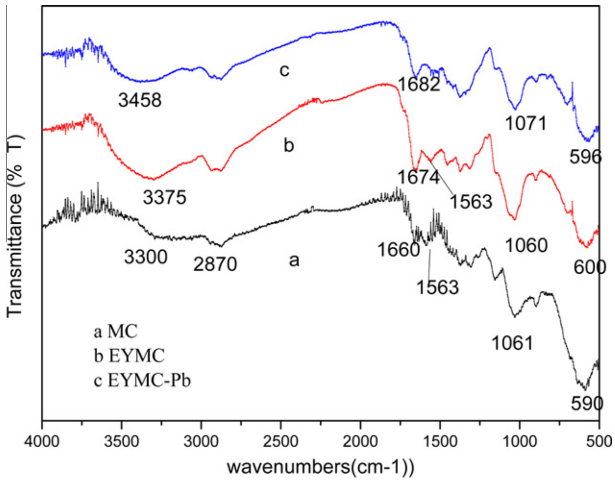

Fig. 2. FTIR spectra for CS (a), EYMC (b), and EYMC-Pb (c) in the region between 500 and 4000 cm^{-1}.

The higher adsorption ability of EYMC may due to the yeast biomass and the ethylenediamine modified on the adsorbents. There are much more adsorption sites (like carboxyl groups and amino groups) on the surface of EYMC after yeast biomass and the ethylenediamine modification, which provide more adsorption sites for ion-exchange and surface complexation. Moreover, the surface charge and the structure of the adsorbent changed after modification.

The four adsorbents showed a low adsorption capacity at the pH 2.0, remarkably increased at the range of 2.0–4.0, and then gently increased from 4.0 to 6.5. This could be accounted for by the pH impacts on the association/dissociation of surface function groups of adsorbents, surface charges, formation of ion species and the interactions between functional group and metal ions [24–26]. When the solution pH was increased from 2.0 to 4.0, the adsorption capacity of EYMC, EMC, YMC, and MC increased from 0.98, 1.16, 0.97, 0.36 mg g^{-1} to 43.1, 33.44, 30.36, 16.89 mg g^{-1}, respectively. This phenomenon was presumably due to the large amount of hydrogen ions at low pH values and their competition for the adsorption sites with Pb^{2+}. On the other hand, at the low pH conditions, the dissociation of functional groups (like carboxyl, amino, and hydroxyl) is difficult. Moreover, the pH_{ZPC} of the EYMC, EMC, YMC, and MC were found to be 5.8, 6.8, 5.3 and 5.6, the four adsorbents were all positively charged at pH < 4.0, leading the electrostatic repulsion occurred between the positive sites and the Pb^{2+} [14,17]. All the above reasons lead the low adsorption efficiency at pH 2.0–4.0.

Within the range of 4.5–6.5, the amount of Pb(II) ions adsorbed to EMC, YMC, and MC slightly increased with the rise of pH, while the adsorption capacity of EYMC had no significant differences (44.10–44.70 mg g^{-1}). This phenomenon presumably because of the weak protonation reaction at high pH value which make more available adsorption sites. Thus, the Pb(II) adsorption could be accomplished through the ion exchange reactions with hydroxyl and carboxyl groups and through the complexation with $-NH_2$ groups [27]. Meanwhile, At the experimental conditions, different complex species could be formed between the Pb^{2+} and Cl^- from HCl, such as $PbCl^+$, $PbCl_2$, $PbCl^{3-}$, and $PbCl_4^{2-}$ [27,28]. The anionic species could be adsorbed on the positive charge of EYMC through the electrostatic attraction. The reduction of the H^+ concentration caused the competition between metal ions and H^+ decreased. As a result, the amount of adsorbed lead ions reached a high level at pH 4.5–6.5. The reasons for the smooth curve of EYMC were probably due to the low concentration of Pb(II) ions. When the pH > 4.0, there was a little metal ions in the solution after adsorption, and the possibility of the collision between metal ions and the functional groups was reduced. Similar trend was observed on the lead adsorption of EDTA-modified magnetic baker's yeast biomass [21]. In order to avoid the formation of $Pb(OH)_2$, pH 5.5 was chosen as the optimum pH value of EYMC and control group in the following experiments.

3.4. Temperature effect on adsorption

To investigate the effect of temperature on the four kinds of adsorbents, experiments were carried out with the initial concentration of 50 mg L^{-1} at three temperatures (20, 30, 40 °C). As shown in Fig. 4, adsorption capacity of the adsorbents increased with the growing temperature. The highest capacity was observed on EYMC at 40 °C (47.61 mg g^{-1}) and the adsorption amounts of the adsorbents were in the following order: EYMC > EMC > YMC > MC, which coincide with the results of pH experiments, probably because of the mobility of Pb^{2+} ions increased at high temperature. Meanwhile, the deprotonation reaction was easy at high temperature, which made more positive groups (amino and

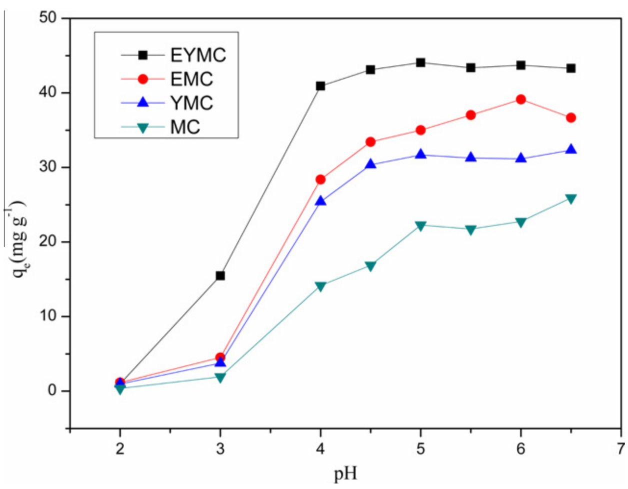

Fig. 3. Effects of pH on adsorption of Pb(II) ions by EYMC and control groups (MC, YMC, and EMC) (initial concentration, 50 mg L^{-1}; volume, 25 mL; absorbent dose, 25 mg; contact time, 1 h; temperature, 30 °C; agitation speed, 150 r min^{-1}).

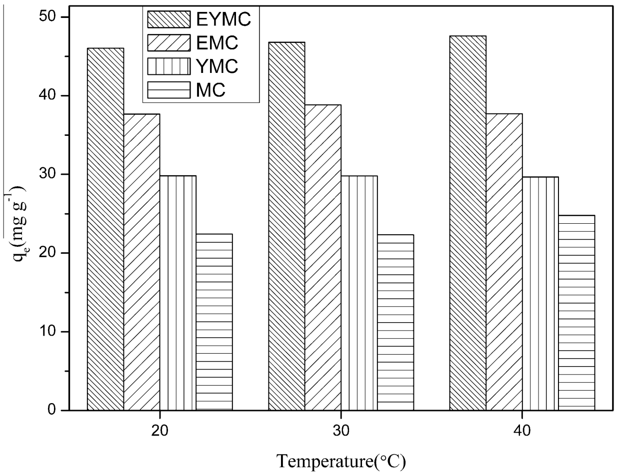

Fig. 4. Effects of temperature on adsorption of Pb(II) ions by EYMC and control groups (MC, YMC, and EMC) (initial concentration, 50 mg L^{-1}; volume, 25 mL; absorbent dose, 25 mg; contact time, 1 h; temperature, 20, 30, 40 °C; pH value, 5.5; agitation speed, 150 r min^{-1}).

carboxyl groups) available for metal removal. And the increasing temperature likely influenced the internal structure of the adsorbents and simplified the ions distribution in the adsorbent's interspaces structure [12].

3.5. Adsorption isotherm studies

Adsorption isotherm studies are necessary to indicate the adsorbent capacity and its surface properties of adsorbents. Many models such as Freundlich and Langmuir were widely utilized to correlate adsorption equilibrium. In this study, Langmuir and Freundlich models were employed to describe the adsorption characteristics between adsorbent and metal ions.

Langmuir model firstly applied for gas molecule adsorption was based on the assumption such as: (1) monomolecular layer adsorption; (2) all adsorption sites are identical and energetically equivalent; (3) each site can accommodate only one molecule or atom; and (4) there is no interaction between adsorbents [12,21,29]. The Langmuir model can be represented as the following equation:

$$q_e = \frac{bq_{\max}C_e}{1 + bC_e} \tag{4}$$

where C_e is the equilibrium concentration of Pb(II) solution (mg L^{-1}); $q_{\max}$ is the maximum adsorption capacity (mg g^{-1}); q_e is the amount of Pb(II) adsorbed per unit weight of adsorbents at equilibrium (mg g^{-1}), b is the equilibrium constant of Langmuir equation (L mg^{-1}).

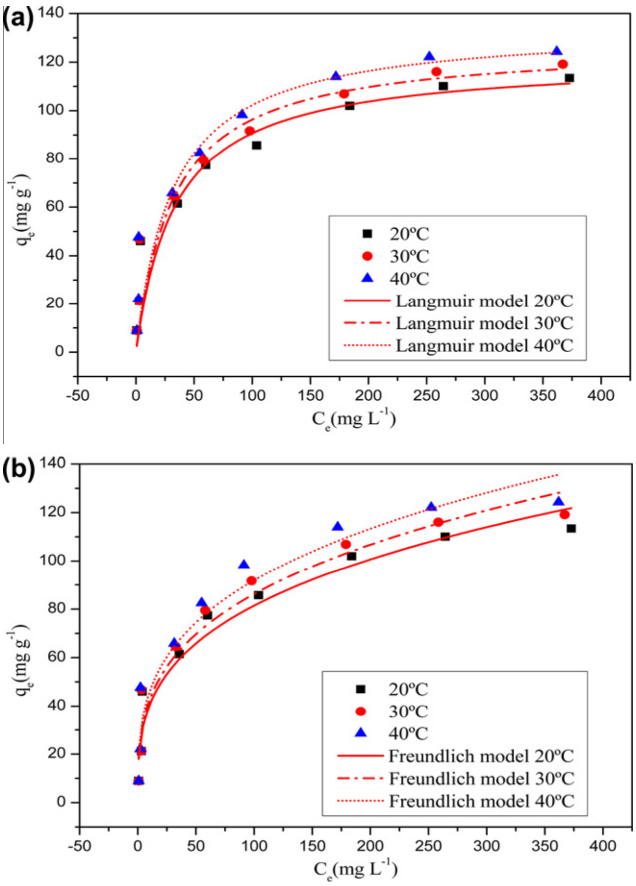

Fig. 5. Langmuir isotherm and Freundlich isotherm for the adsorption of Pb(II) ions on EYMC (initial concentration, 10–500 mg L^{-1}; volume, 25 mL; absorbent dose, 25 mg; contact time, 1 h; temperature, 20, 30, 40 °C; pH value, 5.5; agitation speed, 150 r min^{-1}).

Freundlich isotherm is an empirical equation which considers various kinds of adsorption sites on the solid surface and properly represents the adsorption data at low and intermediate contractions on heterogeneous surfaces. However, the Freundlich model does not consider the adsorbent saturation [30–32]. The equation is defined by the following equation:

$$q_e = K_F C_e^{1/n} \tag{5}$$

where K_F (mg$^{(1-1/n)}$ g^{-1} L$^{1/n}$) and n are the Freundlich constants related to the adsorption capacity and intensity.

The experiment data of Pb(II) adsorption on EYMC were characterized by the Langmuir (Fig. 5a) and Freundlich (Fig. 5b) models. The results were given in Table 1. As shown in Table 1, the experiment data was better described (based on R^2 values) by the Langmuir and Freundlich isotherms. It indicated that monolayer adsorption and heterogeneous surface conditions might coexist under the experimental conditions [32]. Therefore, the adsorption behavior of Pb(II) onto EYMC was complex. It might involve multiple mechanisms, probably ion-exchange, electrostatic attraction and surface complexation [31,33]. The groups like hydroxyl and carboxyl groups could provide ion exchange sites for metal ions [27,34]. The lone pair electrons on N atom of —NH$_2$ groups could bind Pb^{2+} ions or H$^+$ to form a coordination complex through an electron pair sharing [24,27]. Meanwhile, at pH 5.5, the anionic species formed between the Pb^{2+} and Cl$^-$ could be adsorbed on the positive charge of EYMC through the electrostatic attraction [22]. The reaction scheme for the adsorption process can be represented as following. The correlation coefficients for Langmuir (>0.98) and Freundlich (0.92–0.97) indicated that the Langmuir model yields a much better fit than Freundlich model, suggesting monolayer adsorption being more dominant.

$$\mathrm{Pb^{2+} + R{-}OH + H_2O \rightarrow R{-}OPb{-}OH + 2H_3O^+}$$

$$\mathrm{R{-}COOH + Pb^{2+} + H_2O \rightarrow (R{-}COO)_2Pb + H_3O^+}$$

$$\mathrm{R{-}NH_2 + Pb^{2+} + H_2O \rightarrow {-}NH_2(PbOH)^+}$$

$$\mathrm{R{-}NH_3^+ + PbCl^{3-} \rightarrow R{-}NH_3^+PbCl^{3-}}$$

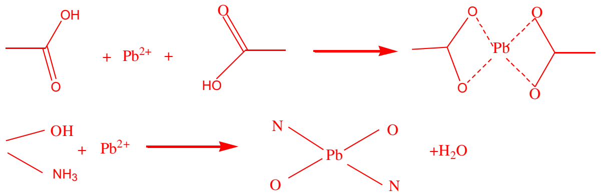

where R represents the surface.

The values of the adsorption capacity $q_{\max}$ and Langmuir constant b were calculated by nonlinear regression and listed in Table 1. The $q_{\max}$ at 20, 30, 40 °C were 121.26, 127.37 and 134.90 mg g^{-1}, b were 2.97×10^{-2}, 3.11×10^{-2}, 3.14×10^{-2} L mg^{-1}, respectively. The increase of $q_{\max}$ indicates the growth of EYMC capacity with the rise of temperature, also reveals that the bonding between the metal ions and functional groups is favorable at higher temperature. This trend is similar to the adsorption of Pb(II) by researcher Zhao et al. [31], The Langmuir constant b indicates the tendency of adsorbent to the metal ions. The greater value indicates the stronger bind of the ions to the adsorbent. It is obvious that EYMC had the highest b values at 40 °C, which is consistent with the $q_{\max}$ obtained by Langmuir model.

The equilibrium data was further analyzed by the Freundlich equation and the values of Freundlich parameters K_F and n were listed at Table 1. As shown in Table 1, with the increase of temperature from 20 to 40 °C both K_F (19.83–21.97 mg$^{(1-1/n)}$ g^{-1} L$^{1/n}$) and

Table 1
Adsorption equilibrium constants obtained from Langmuir and Freundlich isotherms in the adsorption of Pb(II) onto EYMC (initial concentration, 10–500 mg L^{-1}; volume, 25 mL; absorbent dose, 25 mg; contact time, 1 h; temperature, 20, 30, 40 °C; agitation speed, 150 r min^{-1}).

Temperature (°C)	Langmuir			Freundlich		
	q_{max} (mg g^{-1})	b (L mg^{-1})	R^2	K_F ($mg^{(1-1/n)}$ g^{-1} $L^{1/n}$)	n	R^2
20	121.26	2.97×10^{-2}	0.98	19.83	3.26	0.97
30	127.37	3.11×10^{-2}	0.98	20.68	3.25	0.97
40	134.90	3.14×10^{-2}	0.98	21.97	3.89	0.92

n (3.26–3.89) rose, which indicated the growth capacity and intensity of adsorption [35]. This result was consistent with the Langmuir model. It is generally stated that the values of n gives the favorability of adsorption. When the values of n in the range of 2–10, it represent strong adsorption of ions onto the surface of adsorbent, 1–2 moderately difficult, and less than 1 poor adsorption characteristics [36]. From Table 1, the exponent n values were higher than 3 which represented the favorable adsorption condition.

A great deal of workers have experimented several adsorbents for Pb(II) removal. The maximum adsorption capacities of different adsorbents in aqueous solution for Pb(II) ions adsorption were compared in Table 2. It can be seen that the q_m values varies for different adsorbents and that the adsorption capacity of EYMC was higher than other adsorbents except for Chitosan crosslinked with epichlorohydrin-triphosphate (166.94 mg g^{-1}). Although, the q_m of EYMC lower than the adsorbents reported by Laus et al. [37], the adsorption equilibrium time of EYMC (1 h) was far shorter than Chitosan crosslinked with epichlorohydrin-triphosphate (10 h). Thus, the EYMC exhibits a good capacity to remove Pb(II) ions from aqueous.

3.6. Kinetic studies

The effect of the contact time on EYMC adsorption capacity was shown in Fig. 6. The adsorption capacity of EYMC on Pb(II) sharply increased within the first 30 min and no further increase after 1 h. So, only 1 h was required to achieve the equilibrium. The fast Pb(II) removal rate in the first stage might relate to the large numbers of available sites on the surface of EYMC. Moreover, the increase in concentration gradient was also attributed to the fast adsorption. The reason for the slow adsorption process was due to the accumulation of Pb(II) on the surface of EYMC. Furthermore, the decrease of available sites and the concentration gradients lead to the reduction of adsorption at the latter stages [31]. The experiment data of different materials on adsorption had shown a wide range on equilibrium time. According to Laus et al. [37] the Pb(II) adsorption equilibrium time on epichlorohydrin-triphosphate was 12 h. Sun et al. [38] have shown that the crosslinked carboxymethyl-chitosan resin requires 15 h to reach the adsorption equilibrium.

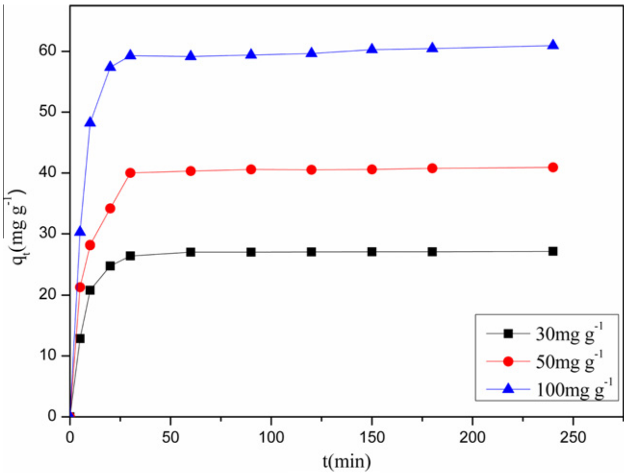

Fig. 6. Effect of contact time on Pb(II) adsorption (initial concentration, 30, 50, 100 mg L^{-1}; volume, 25 mL; absorbent dose, 25 mg; contact time, 1, 5, 10, 20, 30, 60, 90, 120, 150, 180, 240 min; temperature, 30 °C; pH value, 5.5; agitation speed, 150 r min^{-1}).

To investigate the mechanism of adsorption, kinetic models were employed to interpret the experimental data. In this study, pseudo-first-order and pseudo-second-order were applied to analyze the experimental data. The equations of the two different models were expressed as follows.

The pseudo-first-order equation is:

$$\log(q_e - q_t) = \log q_e - \frac{k_1}{2.303}t \quad (6)$$

The pseudo-second-order equation is:

$$\frac{t}{q_t} = \frac{1}{k_2 q_e^2} + \frac{1}{q_e}t \quad (7)$$

where q_e and q_t are the adsorption amount (mg g^{-1}) at equilibrium and at time t, respectively. k_1 is the pseudo-first-order rate constant (min^{-1}), k_2 is the pseudo-second-order rate constant (g mg^{-1} min^{-1}).

Table 2
Pb(II) adsorption capacity of EYMC and some previously used adsorbents.

Adsorbent	Adsorption capacity (mg g^{-1})	$Q_{e,exp}$ (mg g^{-1})	Reference
EYMC	127.37	119.15	This study
Activated tea waste	81	–	[1]
Modified walnut shells	44.48	44.48	[3]
Bacillus sp. ATS-2 immobilized in silica gel	4.89	2.4	[9]
β-MnO_2	16.72	11.5	[26]
GLA-crosslinked metal-complexed chitosans	105.26	–	[29]
Chitosan beads	34.98	7	[33]
Chitosan–GLA beads	14.24	6	[33]
Chitosan–alginate beads	60.27	10	[33]
Chitosan crosslinked with epichlorohydrin-triphosphate	166.94	80	[37]

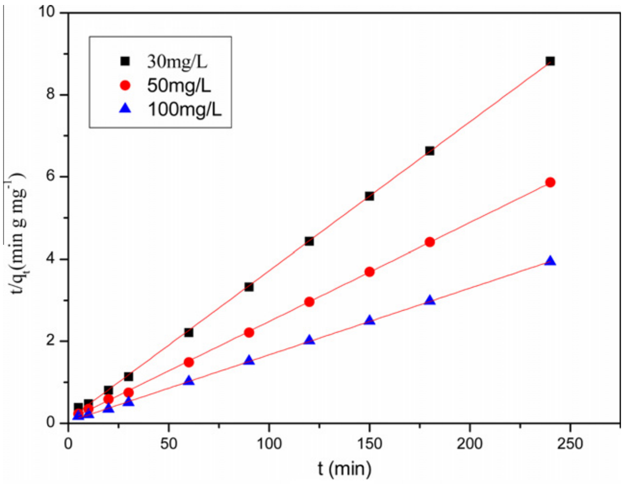

Fig. 7. Pseudo-second-order sorption kinetics of Pb(II) on to EYMC at various initial concentration (initial concentration 30, 50, 100 mg L^{-1}; volume, 25 mL; absorbent dose, 25 mg; contact time, 1, 5, 10, 20, 30, 60, 90, 120, 150, 180, 240 min; temperature, 30 °C; pH value, 5.5; agitation speed, 150 r min^{-1}).

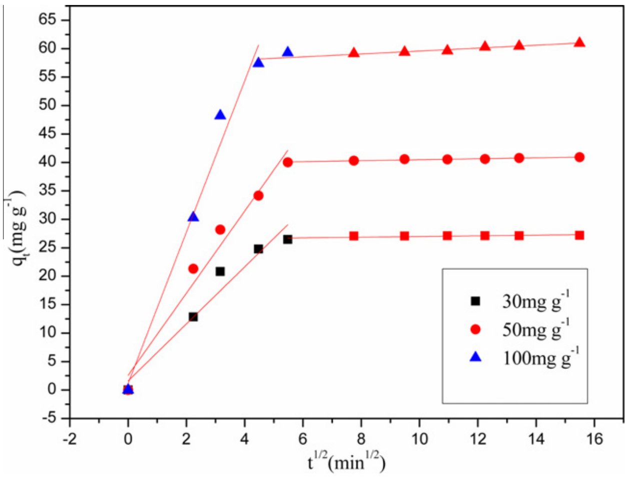

Fig. 8. Intraparticle diffusion kinetics of Pb(II) on to EYMC at various initial concentration (initial concentration, 30, 50, 100 mg L^{-1}; volume, 25 mL; absorbent dose, 25 mg; contact time, 1, 5, 10, 20, 30, 60, 90, 120, 150, 180, 240 min; temperature, 30 °C; pH value, 5.5; agitation speed, 150 r min^{-1}).

The constant k_2 is used to calculate the initial sorption rate h (g mg^{-1} min^{-1}), at $t \to 0$ as follows [33]:

$$h = k_2 q_e^2 \tag{8}$$

Parameters of the pseudo-second-order model were shown in Table 3. It was obvious that the pseudo-second-order equation agreed well with the data for $R^2 > 0.99$. Moreover, the calculated q_e were close to the experimental values. Thus, the pseudo-second-order provided a good correlation for the adsorption of Pb(II) onto EYMC (Fig. 7). Namely, the adsorption process belongs to the second-order model and it fits the assumption behind the model, which suggests the rate limiting step might be chemisorptions involving Valency forces through sharing or exchange of electrons between the adsorption sites and Pb(II) ions [39].

The adsorption process in porous adsorbent can be separated into four steps. The first stage is the movement of metal ions from the bulk liquid to the liquid film surrounding the adsorbent (bulk diffusion). The second one is the diffusion from the film to the surface of the sorbent (film diffusion). The third one is the diffusion in the internal structure of the adsorbent (interparticular diffusion). The fourth one is the solute sorption by complexation or physico-chemical sorption or ion exchange. It is generally accepted that the first and the fourth stage can be ignored. Hence, steps 2 and 3 are the possible rate determining steps [40]. The identification of the diffusion mechanism only by the pseudo-first-order and pseudo-second-order patterns is not practicable. In order to investigate the mechanism and rate controlling steps, intraparticle diffusion model and film diffusion model were applied to obtain insight into the adsorption process.

Intraparticle diffusion equation was given as follows:

$$q_t = k_p t^{1/2} + C \tag{9}$$

where q_t is the amount of metal ions adsorbed at time t (mg g^{-1}), k_p is the intraparticle diffusion rate constant (g mg^{-1} $min^{-0.5}$) and C is the intercept (mg g^{-1}). Intraparticle diffusion should be involved if the curves are straight lines. The intraparticle diffusion is the only rate-limiting step, when the curve passes through the origin. However, if the plots do not pass through the origin, the adsorption process is controlled by some degree of boundary layer [41].

Fig. 8 shows the plot of q_t vs $t^{1/2}$ at different initial concentrations, the parameters were presented in Table 4. It can be seen that all plots were straight lines and do not pass through the origin (the values of C were 1.16–2.26 mg g^{-1}). Meanwhile, the curves have two portions, which suggests that the intraparticle diffusion might be involved but it was not the rate limiting step for the whole reaction. The first portion of the plot indicated an external mass transfer while the other linear portion was due to intraparticle or pore diffusion [42].

To determine the actual rate limiting step, the kinetic data was analyzed using the liquid film diffusion model which was described as follows:

$$\ln(1 - F) = -k_f t \tag{10}$$

$$F = q_t / q_e \tag{11}$$

where k_f (cm s^{-1}) is the film diffusion rate constant and F is the fractional attainment of equilibrium.

When the plot $-\ln(1 - F)$ vs t pass through the origin with zero intercept, it would suggest that the kinetics of the adsorption process is controlled by diffusion through the liquid film [43]. Otherwise it would governed by intraparticle diffusion. As shown in Table 4, the curves were straight lines passing through closely from the origin (the values of intercepts were 0.08, 0.02 and 0.15), which indicated the film diffusion affected the adsorption process. As the intercept were not zero, the resistance was not the only film diffusion. This result was consistent with the intraparticle diffusion model. Usually, film diffusion was the rate limiting step in systems with low concentration of adsorbate, poor mixing, high affinity of

Table 3
Kinetic parameters obtained from kinetic models (initial concentration, 30, 50, 100 mg L^{-1}; volume, 25 mL; absorbent dose, 25 mg; contact time, 1, 5, 10, 20, 30, 60, 90, 120, 150, 180, 240 min; temperature, 30 °C; pH value, 5.5; agitation speed, 150 r min^{-1}).

C_0 (mg L^{-1})	Pseudo-first-order			Pseudo-second-order			
	k_1 (min^{-1})	q_e (mg g^{-1})	R^2	k_2 (g mg^{-1} min^{-1})	q_e (mg g^{-1})	h (mg g^{-1} min^{-1})	R^2
30	0.031	2.15	0.74	0.013	27.60	10.21	>0.99
50	0.027	2.79	0.74	0.007	41.60	12.38	>0.99
100	0.021	3.08	0.66	0.006	61.50	21.76	>0.99

Table 4
Parameters of intraparticle diffusion and film diffusion models (initial concentration 30, 50, 100 mg L^{-1}; volume, 25 mL; absorbent dose, 25 mg; contact time, 1, 5, 10, 20, 30, 60 min; temperature, 30 °C; pH value, 5.5; agitation speed, 150 r min^{-1}).

C_0 (mg L^{-1})	Intraparticle diffusion			Film diffusion		
	k_p (g mg^{-1} $min^{-0.5}$)	C (mg g^{-1})	R^2	k_f (cm s^{-1})	Intercepts	R^2
30	5.01	1.60	0.94	0.118	0.08	0.99
50	7.22	2.26	0.96	0.117	0.02	0.95
100	13.29	1.16	0.97	0.122	0.15	0.98

adsorbents for adsorbents and small adsorbents size. While in those systems with high concentration of adsorbate, good mixing, low affinity of adsorbates for adsorbents and large adsorbents size, the intraparticle step was usually the limiting step [44]. Comparing the parameters of film diffusion and intraparticle diffusion, the rate of adsorption process were mainly governed by the film diffusion.

3.7. Thermodynamic studies

To determine whether the process is spontaneous, both energy and entropy factors were considered. The thermodynamic parameters were calculated by the following equation:

$$\Delta G^\circ = H^\circ - T\Delta S^\circ \tag{12}$$

$$\ln b = \frac{\Delta S^\circ}{R} - \frac{\Delta H^\circ}{RT} \tag{13}$$

$$\Delta G^\circ = -RT\ln b \tag{14}$$

where b is the adsorption equilibrium constant. ΔS°, ΔH° and ΔG° are the changes of entropy (J K^{-1} mol^{-1}), enthalpy (kJ mol^{-1}) and Gibbs energy (kJ mol^{-1}). T (K) is the temperature. R (J mol^{-1} K^{-1}) is the gas constant.

The results of the thermodynamic parameters were shown in Table 5. The negative values for the Gibbs free energy change ΔG° (−21.27, −22.11, −22.86 kJ mol^{-1}) confirmed the process of the adsorption was spontaneous in nature and the degree of the reaction spontaneity increased with the rising temperature [12]. The absolute value of ΔG° increased probably related to the ascending number of the active sites which are available for adsorption process and the decrease of the boundary layer surrounding the adsorbent [45].

The positive value of ΔH° (2.11 kJ mol^{-1}) indicated that the adsorption process is endothermic. This might attribute to the deprotonation reaction and the diffusion process. Deprotonation reactions were easy at high temperature. Meanwhile, diffusion process was an endothermic process, the rate of the process rose with the increasing temperature. This was in agreement with the increasing $q_{\max}$ and n obtained in the Langmuir and Freundlich model (Table 1).

The positive value of ΔS° (79.78 J K^{-1} mol^{-1}) reflects the growth of randomness at the solid/solution interface and a good affinity of Pb(II) towards EYMC. This is due to the structural changes of adsorbate and adsorbent during the adsorption, which made the increase in the disorderness of the solid/solution system [46].

Table 5
Thermodynamic parameters for the adsorption of Pb(II) ions by EYMC (initial concentration, 10–500 mg L^{-1}; volume, 25 mL; absorbent dose, 25 mg; contact time, 1 h; temperature, 20, 30, 40 °C; pH value, 5.5; agitation speed, 150 r min^{-1}).

ΔH° (kJ mol^{-1})	ΔS° (J K^{-1} mol^{-1})	ΔG° (kJ mol^{-1})		
		20 °C	30 °C	40 °C
2.11	79.78	−21.27	−22.11	−22.86

Table 6
Adsorption-desorption cycles for EYMC.(adsorption conditions: initial concentration, 50 mg L^{-1}; volume, 25 mL; absorbent dose, 25 mg; contact time, 1 h; temperature, 30 °C,; pH value, 5.5; agitation speed, 150 r min^{-1}. Desorption conditions: volume, 25 mL of 0.1 M EDTA; contact time, 1 h; temperature, 30 °C.).

	Pb(II) ions absorbed (mg g^{-1})	Desorption (%)	Adsorption efficiency (%)
1	45.81	98.43	93.07
2	45.67	95.82	92.79
3	45.40	94.36	92.24
4	45.20	95.44	92.10

3.8. Desorption studies

The repeated availability of the adsorbents after adsorption–desorption cycles is crucial to illustrate the stability and potential recovery of the adsorbents. In this investigation, consecutive regenerations for EYMC at elution solution of 0.1 M EDTA were shown in Table 6. The desorption efficiency decreased from 98.4% to 94.4% in the first three cycles and increased to 95.4% in the last one. Desorption by EDTA solution easily occurred might be related to the intensive competition between H^+ ions (introduced by EDTA solution) and metal ions on the active sites. Meanwhile, at low pH value, the complexation between the adsorbent and metal ions was destroyed [47,48]. Thus, Pb(II) ions could be desorbed from the adsorbents. The adsorption capacity of EMYC decreased a little (0.61 mg g^{-1}) after four times of adsorption–desorption cycles. These results illustrated that the EYMC possess the ability of regeneration and repeated use in heavy metal removal with slight losses in their initial adsorption capacities.

4. Conclusions

Comparing with MC, EMC and YMC, EYMC showed its effective ability in removing Pb(II) from water. Adsorption capacity of EYMC for Pb(II) was found higher in a wide range of pH (4.0–6.0) and the amount of adsorbed metal ions increase with rising pH. The experiment data was well described by the Langmuir and Freundlich isotherms, while Langmuir model illustrated the best description with its higher R^2. It indicated that monolayer adsorption and heterogeneous surface conditions may coexist, while monolayer adsorption being more dominant. The maximum adsorption capacity obtained from Langmuir model were 121.26, 127.37 and 134.90 mg g^{-1} at 20, 30 and 40 °C, respectively. Kinetic studies showed that the pseudo-second-order model was appropriate to describe the adsorption process of EYMC and film diffusion maybe governed the rate of the adsorption. Kinetic studies also suggested the rate limiting step may be chemisorption. Parameters from thermodynamic studies (ΔG° and ΔH°) showed that the adsorption of Pb(II) onto EYMC was a spontaneous process and endothermic in nature. The stability and potential recovery of the EYMC were proved by the adsorption–desorption cycles. Consequently, the experimental results suggest that EYMC will have broad applications in the removal of Pb(II) ions from aqueous solution.

References

[1] M.K. Monda, Removal of Pb(II) ions from aqueous solution using activated tea waste: adsorption on a fixed-bed column, J. Environ. Manage. 90 (2009) 3266–3271.

[2] D. Mohan, K.P. Singh, Single and multicomponent adsorption of cadmium and zinc using activated carbon derived from bagasse an agricultural waste, Water Res. 36 (2002) 2304–2318.

[3] S. Saadat, A. Karimi-Jashni, Optimization of Pb(II) adsorption onto modified walnut shells using factorial design and simplex methodologies, Chem. Eng. J. 173 (2011) 743–749.

[4] R.M. Perez Silva, A. Abalos Rodriguez, J.M. Gomez Montes De Oca, D. Cantero Moreno, Biosorption of chromium, copper, manganese and zinc by *Pseudomonas aeruginosa* AT18 isolated from a site contaminated with petroleum, Bioresour. Technol. 100 (2009) 1533–1538.

[5] E.S. Cossich, C.R. Granhen Tavares, T.M. Kakuta Ravagnani, Biosorption of chromium(III) by *Sargassum* sp. biomass, Electron. J. Biotechnol. 5 (2002) 133–140.

[6] H. Krheminska, D. Fedorovych, L. Babyak, D. Yanovych, P. Kaszycki, H. Koloczek, Chromium(III) and (VI) tolerance and bioaccumulation in yeast: a survey of cellular chromium content in selected strains of representative genera, Process Biochem. 40 (2005) 1565–1572.

[7] M.X. Loukidou, K.A. Matis, A.L. Zouboulis, M.L. Kyriakidou, Removal of As(V) from wastewaters by chemically modified fungal biomass, Water Res. 37 (2003) 4452–4544.

[8] T. Akar, Z. Kaynak, S. Ulusoy, D. Yuvaci, Enhanced biosorption of nickel(II) ions by silica-gel-immobilized waste biomass: biosorption characteristics in batch and dynamic flow mode, J. Hazard. Mater. 163 (2009) 1134–1141.

[9] A. Cabuk, T. Akar, S. Tunali, O. Tabak, Biosorption characteristics of *Bacillus* sp. ATS-2 immobilized in silica gel for removal of Pb(II), J. Hazard. Mater. B. 136 (2006) 317–323.

[10] A. Witek-Krowiak, R.G. Szafran, S. Modelski, Biosorption of heavy metals from aqueous solutions onto peanut shell as a low-cost biosorbent, Desalination 265 (2011) 126–134.

[11] P.A. Marques, H.M. Pinheiro, J.A. Teixeira, M.F. Rosa, Removal efficiency of Cu^{2+}, Cd^{2+} and Pb^{2+} by waste brewery biomass: pH and cation association effects, Desalination 124 (1999) 137–144.

[12] Y. Tian, C. Jin, M. Zhao, M. Xu, Y.S. Zhang, Preparation and characterization of baker's yeast modified by nano-Fe$_3$O$_4$: application of biosorption of methyl violet in aqueous solution, Chem. Eng. J. 165 (2010) 474–481.

[13] B. Volesky, H. May, Z.R. Holan, Cadmium biosorption by *Saccharomyces cerevisiae*, Biotechnol. Bioeng. 41 (1993) 826–829.

[14] A. Kapoor, T. Viraraghavan, D.R. Cullimore, Removal of heavy metals using the fungus *Aspergillus niger*, Bioresour. Technol. 70 (1999) 95–104.

[15] R.S. Sudha, T.E. Abraham, Studies on enhancement of Cr(VI) biosorption by chemically modified biomass of *Rhizopus nigricans*, Water Res. 36 (2002) 1224–1236.

[16] J. Knaul, M. Hooper, C. Chanyi, K.A.M. Creber, Improvements in the drying process for wet-spun chitosan fibers, J. Appl. Polym. Sci. 69 (1998) 1435–1444.

[17] A. Ramesh, H. Hasegawa, W. Sugimoto, T. Maki, K. Ueda, Adsorption of gold(III), platinum(IV) and palladium(II) onto glycine modified crosslinked chitosan resin, Bioresour. Technol. 99 (2008) 3801–3809.

[18] E.B. Denkbas, E. Kilicay, C. Birlikseven, E. Öztürk, Magnetic chitosan microspheres: preparation and characterization, React. Funct. Polym. 50 (2002) 225–232.

[19] M. Rutnakornpituk, P. Ngamdee, P. Phinyocheep, Preparation and properties of polydimethylsiloxane-modified chitosan, Carbohydr. Polym. 63 (2006) 229–237.

[20] Z.L. Bao, J.S. Wang, J.H. Liu, L.P. Liu, Preparation of water-based Fe$_3$O$_4$ magnetic fluids via chemical co-precipitation as precursors of complex adsorbent, in: 2009 International Symposium on Environmental Science and Technology, Shanghai, China, June 2–5, 2009, pp. 1585–1591.

[21] M. Xu, Y.S. Zhang, Z.M. Zhang, Y. Shen, Study on the adsorption of Ca^{2+}, Cd^{2+} and Pb^{2+} by magnetic Fe$_3$O$_4$ yeast treated with EDTA dianhydride, Chem. Eng. J. 168 (2011) 737–745.

[22] L. Zhou, Z. Liu, J. Liu, Q. Huang, Adsorption of Hg(II) from aqueous solution by ethylenediamine-modified magnetic crosslinking chitosan microspheres, Desalination 258 (2010) 41–47.

[23] K. Sufia, K. Kazy Susanta, S. Das Pinaki, Lanthanum biosorption by a Pseudomonas sp.: equilibrium studies and chemical characterization, J. Ind. Microbiol. Biotechnol. 33 (2006) 773–783.

[24] G.Y. Li, K.L. Huang, Y.R. Jiang, D.L. Yang, P. Ding, Preparation and characterization of Saccharomyces cerevisiae alcohol dehydrogenase immobilized on magnetic nanoparticles, Int. J. Biol. Macromol. 42 (2008) 405–412.

[25] J. Li, R.B. Bai, Mechanisms of lead adsorption on chitosan/PVA hydrogel beads, Langmuir 18 (2002) 9765–9770.

[26] D. Zhao, X. Yang, H. Zhang, C. Chen, X. Wang, Effect of environmental conditions on Pb(II) adsorption on β-MnO2, Chem. Eng. J. 164 (2010) 49–55.

[27] J. Zhu, J. Yang, B. Deng, Ethylenediamine-modified activated carbon for aqueous lead adsorption, Environ. Chem. Lett. 8 (2010) 277–282.

[28] J. Rivera-Utrilla, I. Bautista-Toledo, M.A. Ferro-Garcia, C. Moreno-Castilla, Activated carbon surface modifications by adsorption of bacteria and their effect on aqueous lead adsorption, J. Chem. Technol. Biotechnol. 76 (2001) 1209–1215.

[29] A.H. Chen, C.Y. Yang, C.Y. Chen, C.Y. Chen, C.W. Chen, The chemically crosslinked metal-complexed chitosans for comparative adsorptions of Cu(II), Zn(II), Ni(II) and Pb(II) ions in aqueous medium, J. Hazard. Mater. 163 (2009) 1068–1075.

[30] X.L. Tan, X.K. Wang, M. Fang, C.L. Chen, Sorption and desorption of Th(IV) on nanoparticles of anatase studied by batch and spectroscopy methods, Colloid Surf. A. 296 (2007) 109–116.

[31] D. Zhao, G. Sheng, J. Hu, C. Chen, X. Wang, The adsorption of Pb(II) on Mg$_2$Al layered double hydroxide, Chem. Eng. J. 171 (2011) 167–174.

[32] A. Ozcan, A.S. Ozcan, S. Tunali, T. Akar, I. Kiran, Determination of the equilibrium, kinetic and thermodynamic parameters of adsorption of copper(II) ions onto seeds of *Capsicum annuum*, J. Hazard. Mater. 124 (2005) 200–208.

[33] W.S. Wan Ngah, S. Fatinathan, Pb(II) biosorption using chitosan and chitosan derivatives beads: equilibrium, ion exchange and mechanism studies, J. Environ. Sci. 22 (2010) 338–346.

[34] A.J. Varma, S.V. Deshpande, J.F. Kennedy, Metal complexation by chitosan and its derivatives: a review, Carbohydr. Polym. 55 (2004) 77–93.

[35] Z. Aksu, O. Tunc, Application of biosorption for penicillin G removal: comparison with activated carbon, Process Biochem. 40 (2005) 831–847.

[36] R.E. Treybal, Mass-transfer Operations, third ed., McGraw-Hill, 1981.

[37] R. Laus, T.G. Costa, B. Szpoganicz, V.T. Fávere, Adsorption and desorption of Cu(II), Cd(II) and Pb(II) ions using chitosan crosslinked with epichlorohydrin-triphosphate as the adsorbent, J. Hazard. Mater. 183 (2010) 233–241.

[38] S. Sun, L. Wang, A. Wang, Adsorption properties of crosslinked carboxymethyl-chitosan resin with Pb(II) as template ions, J. Hazard. Mater. B 136 (2006) 930–937.

[39] C. Septhum, S. Rattanaphani, J.B. Bremner, V. Rattanaphani, An adsorption study of Al(III) ions onto chitosan, J. Hazard. Mater. 148 (2007) 185–191.

[40] W.H. Cheung, Y.S. Szeto, G. McKay, Intraparticle diffusion processes during acid dye adsorption onto chitosan, Bioresour. Technol. 98 (2007) 2897–2904.

[41] A. Ozcan, A.S. Ozcan, Adsorption of Acid Red 57 from aqueous solutions onto surfactant-modified sepiolite, J. Hazard. Mater. 125 (2005) 252–259.

[42] J. Aguilar-Carrillo, F. Garrido, L. Barrios, M.T. Garcia-Gonzalez, Sorption of As, Cd and Tl as influenced by industrial by-products applied to an acidic soil: equilibrium and kinetic experiments, Chemosphere 65 (2006) 2377–2387.

[43] A.R. Iftikhar, H.N. Bhatti, M.A. Hanifa, R. Nadeem, Kinetic and thermodynamic aspects of Cu(II) and Cr(III) removal from aqueous solutions using rose waste biomass, J. Hazard. Mater. 161 (2009) 941–947.

[44] V. Vadivelan, K.V. Kumar, Equilibrium, kinetics, mechanism, and process design for the sorption of methylene blue onto rice husk, J. Colloid Interface Sci. 286 (2005) 90–100.

[45] E. Eren, H. Gumus, A. Sarihan, Synthesis structural characterization and Pb(II) adsorption behavior of K- and H-birnessite samples, Desalination 279 (2011) 75–85.

[46] Q.H. Fan, X.L. Tan, J.X. Li, X.K. Wang, W.S. Wu, G. Montavon, Sorption of Eu(III) on attapulgite studied by batch, XPS and EXAFS techniques, Environ. Sci. Technol. 43 (2009) 5776–5782.

[47] M.R. Huang, H.J. Lu, X.G. Li, Efficient multicyclic sorption and desorption of lead ions on facilely prepared poly (m-phenylenediamine) particles with extremely strong chemoresistance, J. Colloid Interface Sci. 313 (2007) 72–79.

[48] Y. Ren, N. Li, J. Feng, T. Luan, Adsorption of Pb(II) and Cu(II) from aqueous solution on magnetic porous ferrospinel MnFe$_2$O$_4$, J. Colloid Interface Sci. 367 (2011) 415–421.